Dalton Transactions

Accepted Manuscript

ROYAL SOCIETY OF CHEMISTRY

www.rsc.org/dalton

Cite this: DOI: 10.1039/c0xx00000x

www.rsc.org/xxxxxx

ARTICLE TYPE

Encapsulation of Large Dye Molecules in Hierarchically Superstructured Metal-Organic Frameworks

Yanfeng Yue,[a] Andrew J. Binder,[b] Ruijing Song,[c] Yuanjing Cui,[*c] Jihua Chen,[d] Dale K. Hensley,[d] and Sheng Dai[*ab]

Received (in XXX, XXX) Xth XXXXXXXXX 20XX, Accepted Xth XXXXXXXXX 20XX
DOI: 10.1039/b000000x

Microporous metal–organic frameworks (MOFs) represent a new family of microporous materials, offering potential applications in gas separation and storage, catalysis, and membranes. The engineering of hierarchical superstructured MOFs, i.e., fabricating mesopores in microporous frameworks during the crystallization stage is expected to serve a myriad of applications for molecular adsorption, drug delivery, and catalysis. However, MOFs with mesopores are rarely studied because of the lack of a simple, effective way to construct mesoscale cavities in the structures. Here, we report the use of a perturbation-assisted nanofusion technique to construct hierarchically superstructured MOFs. In particular, the mesopores in the MOF structure enabled the confinement of large dye species, resulting in fluorescent MOF materials, which can serve as a new type of ratiometric luminescent sensors for typical volatile organic compounds.

Introduction

Metal-organic frameworks (MOFs) are a new development on the interface between molecular coordination chemistry and materials science. They are hybrid inorganic–organic crystalline solids in which secondary building units (SBUs) are assembled to form a periodic and porous framework, which is strongly dependent on the coordination preference of the metal ion and the length and rigidity of the oligotopic organic linkers.[1–4] This new class of porous materials has attracted a tremendous amount of interest because of its fascinating structural topologies, high surface area, and potential in applications such as gas storage, gas purification, catalysis, and sensing.[5,6]

Despite the success of MOFs in gas storage and separation, difficulties associated with the transport of large molecules across narrow pores inside the MOF structure limit their applications for anchoring molecular catalysts, impregnation with catalyst precursors, or large molecule adsorption. Therefore, hierarchically structured porous MOFs, created by embedding mesopores in classical microporous skeletons, have become a topic of intense interest because of the short diffusion pathways resulting from the textural mesopores and more exposed coordination metal sites.[7] However, the investigation of MOFs with a hierarchical structure of micropores and mesopores is still in its infancy, and the augmentation of their channel sizes to the mesoporous range still poses a challenge. Significant efforts are therefore being undertaken to construct MOF mesopores in MOFs to confine functional species, especially for large molecules, leading to specific behavior inside the defined pore environments.[8–10] Previously, much effort has been devoted to the synthesis of hierarchical MOFs. State-of-the-art MOF hierarchical materials can be categorized into two types: those prepared by ligand extension and those prepared using a template. In the former case, MOF materials exhibit mesoporous behavior as a result of intrinsic mesopores throughout their structures meticulously formed by extending linear organic linkers.[11] However, the development of such mesoporous frameworks by ligand extension is challenging, because expanded frameworks are often more fragile leading to a collapse of the framework during removal of included guests molecules. At the same time, attempts to construct mesoporous MOFs by ligand extension often yield either interpenetrating structures, which dramatically reduce the size of the pore aperture. The template method, which uses organic molecules as templates, is widely used to prepare various mesoporous metal oxides and silicas.[12]

An alternative method to fabricate mesopores in MOF structures is to construct porous superstructures with nanocrystal building units. Recently, MOFs with an extended mesoporous superstructure were obtained through a cooperative template method that uses a surfactant and a chelating agent. The surfactant molecules form micelles, and the chelating agent bridges the micelles, i.e., templating the mesopore formation and directing the crystal growth.[13] However, the template directing strategy for preparation of hierarchical MOF superstructures has the disadvantage of requiring removal of the template, which might damage the implemented mesopores. Furthermore, template-directing synthesis is somewhat cost- and time-intensive because of the template, and it is not environmentally friendly. Thus it is not only challenging but also important to build hierarchically superstructured MOF materials without a templating agent.

In the absence of a templating agent, the first question in mesoporous superstructure construction is how to generate SBUs that do not assemble into large single crystals. To accomplish this, upon the addition of the organic ligand into the metal ion precursor solution, the mixture was stirred vigorously. This process avoids the formation of large MOF single crystals that would occur without the perturbation. In detail, when the deprotonation of the organic linkers was impacted, SBUs were formed and further aggregated into nanosize MOF particles in

which the scaffolding framework was fabricated by metal–ligand coordination. The nanosize MOF crystals were potential sources for the formation of mesopores through a "nanofusion" mechanism, previously used to fabricate porous silica and electrode materials: the discrete nanosize MOF crystals were embedded in an amorphous matrix, and mesopores formed spontaneously.[14] The next question is how to balance the speed of crystallization and nanofusion growth. This process is elusive and difficult to control, because crystallization of the nanosize MOF particles requires—in conjunction with other supramolecular interactions such as hydrogen bonding and π-π stacking—a dissociation–recoordination force for forming the "interunit" bridges on which the nanofusion technique depends. So it is important to choose the proper solvent to control the speed of crystallization. At the same time, strong stirring is beneficial to nanofusion growth because it prevents the ordered growth of the crystal. This perturbation-assisted methodology for fabricating hierarchical superstructures of MOFs through critical control over self-assembled nanosize building blocks was termed the "perturbation-assisted nanofusion" technique (**Scheme 1**).

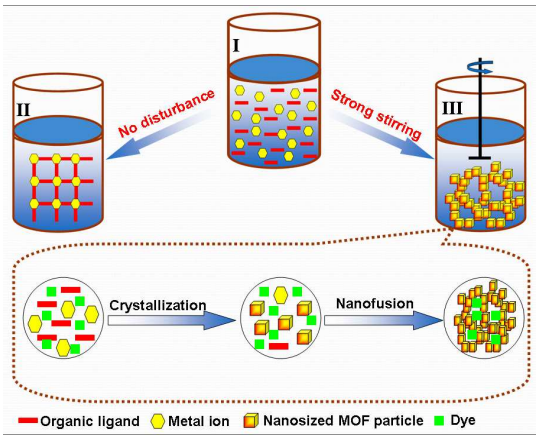

Scheme 1. Schematic illustration of perturbation-assisted nanofusion mechanism for the formation of hierarchical superstructure of MOFs, with large dye molecules simultaneous entrapment. (I, initial state with ligands and metal ions dispersed in the solution; II, big single crystals with ordered structure obtained without any perturbation; III, hierarchical superstructure fabricated under strong stirring).

Results and discussions

Herein, we demonstrated perturbation-assisted nanofusion to prepare a series of MOF materials with hierarchical superstructure: IRMOF-3 ($Zn_4O(NH_2BDC)_3\cdot(guest)_n$, where NH_2BDC is 2-amino-1,4-benzenedicarboxylate);[15] Cu-BDC ($Cu(BDC)\cdot(guest)_n$, where BDC is 1,4-benzenedicarboxylate);[16] Cu-BTEC ($Cu_2(BTEC)\cdot(guest)_n$, where BTEC is 1,2,4,5-benzenetetracarboxylate).[17] These include most of the known MOF subfamilies and related mesopores fabricated in the structures. In all cases, the hierarchical superstructured MOF materials retain the excellent structures of the parent materials. In particular, based on this template-free perturbation-assisted nanofusion technique, RB@IRMOF-3 composite (RB = Rhodamine B) was fabricated with gram-scale product instantly. Interestingly, the luminescence study suggested the dye@MOF composite can serve as a new type of ratiometric luminescent sensors for typical volatile organic compounds (VOCs).

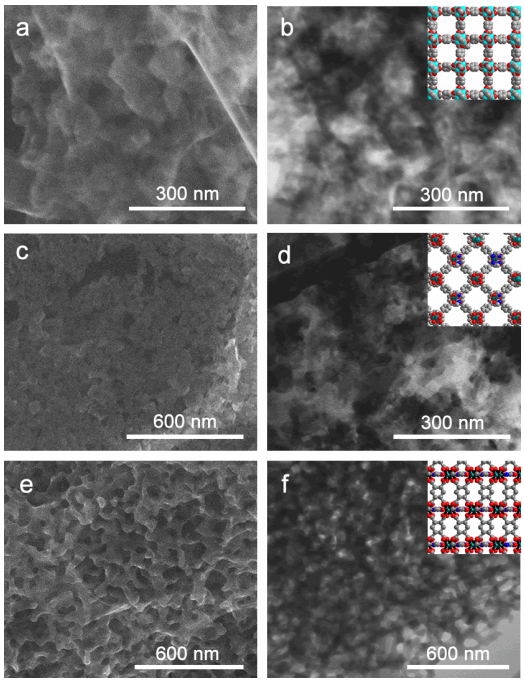

Figure 1. SEM (a, IRMOF-3; c, Cu-BDC; e, Cu-BTEC), TEM (b, IRMOF-3; d, Cu-BDC; f, Cu-BTEC) images, and crystal structure of related MOF with guests molecules omitted for clarity (inset).

The XRD patterns of these hierarchical MOF materials matched well with patterns simulated for single-crystal data (Figure S1, Supporting Information, SI). **Figure 1** presents typical SEM and TEM images of the resulting hierarchical superstructures, in which pores are constructed from irregular particles. As observed in the SEM image, continuous networks of nanosize particles formed, with discrete nanosize crystals embedded in an amorphous matrix with disordered mesopores, in the range of 5–40 nm for IRMOF-3, Cu-BDC and Cu-BTEC. The pore structure was also investigated through TEM analysis. However, the pores are distributed randomly, giving wormhole-like disordered mesostructures for IRMOF-3, Cu-BDC and Cu-BTEC.

Further characterization by nitrogen physical adsorption confirmed the surface areas, pore sizes, and pore volumes. A typical type IV isotherm with an H2 hysterisis loop could be observed for IRMOF-3, Cu-BDC and Cu-BTEC, indicating the mesoporous nature of these samples. Pronounced desorption hyteresis suggests the existence of mesopores in these materials. The Barrett-Joyner-Halenda (BJH) pore-size distribution curves (PSD) indicate the mesopores of these MOF materials approximate in the range of 5–40 nm in diameter, well matched with the detection of the TEM images. Compared with the microporous parent MOFs, the BET surface areas of these hierarchical MOFs are reduced (**Figure 2** and Table S1, SI). This is reminiscent of the amorphous nature of the pore walls or collapse of the mesostructure upon the removal of guest molecules. We note that, on the one hand, this method of preparing mesoporous MOFs guarantees that the framework structure is not altered, because the precipitated material is composed of discrete nanosize MOF particles; and, on the other hand, the hierarchical porous superstructure is obtained from the self-assembly of highly monodispersed nanosize MOF particles which are embedded in an amorphous matrix.[18] Furthermore, the perturbation played a predominant role in the formation of

mesopores because it accelerated the growth speed of crystallites to balance the speed of crystallization.

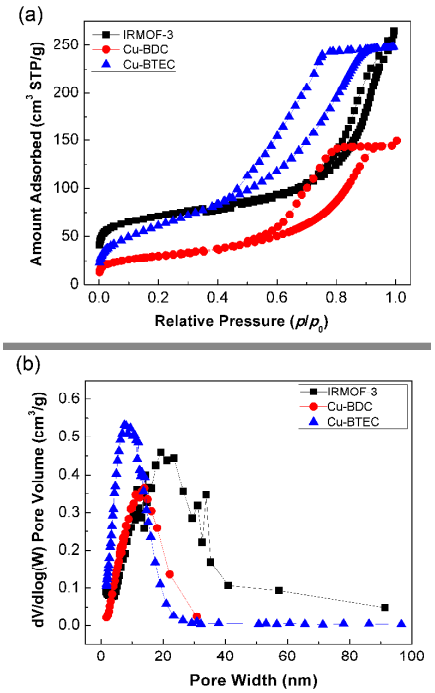

Figure 2. N_2 –196 °C isotherms of IRMOF-3, Cu-BDC, and Cu-BTEC, and corresponding Barrett-Joyner-Halenda (BJH) pore-size distribution curves (PSD) (b).

We envisaged that by dissolving dye molecules in one of the precursor solutions before mixing, we should be able to extend the perturbation-assistant nanofussion approach to achieve simultaneous entrapment of large dye species inside the nanosize pores of the superstructures. In fact, the introduction of fluorescent dyes into MOF pore spaces always uses a time-consuming diffusion or ion exchange method.[19] At the same time, the encapsulation based on diffusion method will not be achieved when the volume of the dye larger than the pores of the MOFs. Therefore, our perturbation-assistant nanofussion technique would enable the confinement of large molecules of the dye species because the dye molecules can be physically encapsulated in the mesopores during the preparation process.

Rhodamine B (1.6 nm molecular diameter)[20] molecules were used as a fluorescent dopant without any chemical modification for covalent linking, providing for successful fixing of the large dye molecules into the hierarchical MOF materials. RB is widely used as a colorant in textiles and food stuffs and is a well-known water tracer fluorescent because of its strong absorption and very high fluorescence quantum yield.[21] The XRD patterns of dye-encapsulated MOF (RB@IRMOF-3) composite matched well with patterns simulated for single-crystal data (Figure S2, SI). The specific surface area of the dye-encapsulated composite was also determined by N_2 adsorption–desorption measurement. The rapidly increasing adsorption volume at very low relative pressure and a typical type IV isotherm with an H2 hysterisis loop in the high relative pressure were observed (Figure S3, SI), indicating the presence of micropores in the crystalline nanosized building blocks and the existence of textural meso/macropores formed by aggregation the nanosized particles. Pronounced micropores in the composite material (Table S1, SI), may be due to the addition of RB molecules affects the speeds of crystallization and nanofusion growth.

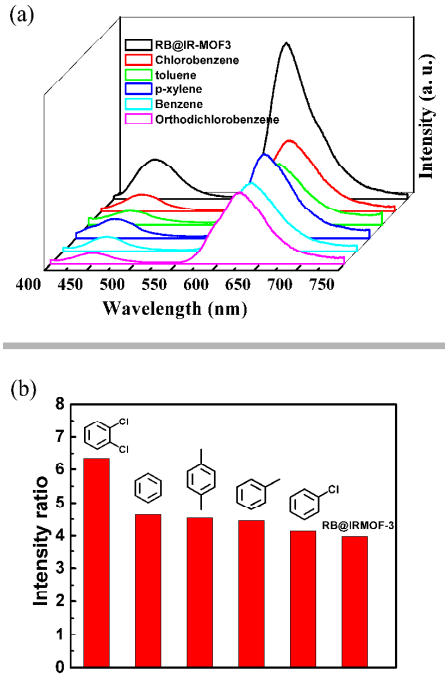

Figure 3. Fluorescence spectra of RB@IRMOF-3 (a) and the emission peak-height ratios between ligand and dye moieties in RB@IRMOF-3 (b).

As shown in Figure S4, the RB solution in ethanol (10^{-5} mol L^{-1}) exhibited the characteristic emission at 570 nm when excited at 355 nm, while the dye-encapsulated MOF RB@IRMOF-3 simultaneously displayed the characteristic emissions of both the RB dye and the MOF after excitation at 355 nm in the solid state. The weak and broad band peaking at 450 nm in the emission spectrum is attributed to the π-π* electron transition of the ligand, while the red emission band around 605 nm originated from the RB dye. The red-shift of the emission of RB in hierarchical IRMOF-3 should be attributed to the increased polarity in IRMOF-3. This indicates that that the large RB dye molecules had been successfully encapsulated into the hierarchical IRMOF-3, which is not possible instantly for the encouterpart microporous IRMOF-3 which has substantially smaller pore apertures (8 Å).[22] Other dye molecules, such as methyl orange, methylene blue and perylene, were also tried to encapsulate in hierarchically superstructured IRMOF-3. However, these dye molecules always leak out from the MOF material, possibly because of the weak interactions between the dye guest molecules and the framework.

In order to study potential applications of the two-color ratiometric emission of the RB@IRMOF-3 composite in sensors, the luminescence was studied after treating with typical volatile organic compounds (VOCs) such as orthodichlorobenzene, chlorobenzene, benzene, toluene, p-xylene, methanol, and ethanediol (**Figure 3a**). After exposure to orthodichlorobenzene, the luminescence peak of the RB@IRMOF-3 at 450 nm and 606 nm exhibited a red-shift, while treated with chlorobenzene, benzene, toluene, p-xylene, only the luminescence peak of at 606 nm exhibited a red-shift. As shown in **Figure 3b**, the values of intensity ratio between ligand and dye moieties were 4.14, 4.45, 4.54, 4.63 and 6.35 for chlorobenzene, toluene, *p*-xylene, benzene, orthodichlorobenzene, respectively, which increase compared with RB@IRMOF-3. The RB@IRMOF-3 after exposure to methanol and ethanediol, the emission intensity of ligand increased, while the emission intensity of rhodamine moieties decreased, and the values of intensity ratio between ligand and

dye moieties has a significantly decrease, being 0.67 and 0.53, respectively. However, treated with methanol, the luminescence peak at 450 nm and 606 nm exhibited a red-shift, and treated with ethanediol, the luminescence peak at 450 nm exhibited a blue-shift and the luminescence peak at 606 nm exhibited a red-shift (Figure S5, S6). The inclusion of different solvent molecules within the MOF channels maybe affect the host–guest energy transfer efficiency between the host matrix and the guest molecules, suggesting that RB@IRMOF-3 composite can serve as a new type of ratiometric luminescent sensors for VOCs.

Conclusions

We have presented and illustrated a perturbation-assisted nanofusion technique for fabricating MOF materials with a hierarchical superstructure. A key to this methodology for designing the superstructure lies in the fabrication of ultrasmall nanocrystals (a few nanometers in size) and the subsequent assembly of these nanocrystal building units into interconnected porous frameworks while preventing their growth into large single crystals by perturbation—a synergistically coupled nanocrystal formation and aggregation mechanism. More importantly, this template-free methodology allows the preparation of stable MOF materials with mesopores, which is difficult to accomplish by organic ligand extension. Furthermore, this method stands as an environmentally friendly and low-cost alternative to hard or soft templating for the fabrication of mesoporous materials beyond MOFs, thereby opening up new avenues for the design of more sophisticated, hollow superstructures, particularly for materials with lower chemical and physical stability.

The mesopores in the MOF structure enabled the simultaneous confinement of large molecules of dye species during the formation of the superstructures, resulting in fluorescent MOF composite materials. The luminescence studies suggested the dye in the hierarchical superstructure can serve as a new type of ratiometric luminescent sensors for typical volatile organic compounds. This should facilitate the development and exploitation of MOFs for numerous applications, including drug delivery, pollutant removal, storage and separation, catalysis, sensor technology, capsules, reactors, and highly complex composites.

Acknowledgement

This research was sponsored by the Division of Chemical Sciences, Geosciences, and Biosciences, Office of Basic Energy Sciences, US Department of Energy, under Contract DE-AC05-00OR22725 with Oak Ridge National Laboratory, which is managed and operated by UT-Battelle, LLC. A portion of this research was conducted at the Center for Nanophase Materials Sciences, which is sponsored at Oak Ridge National Laboratory by the Division of Scientific User Facilities, Office of Basic Energy Sciences, US Department of Energy.

Notes and references

[a]*Chemical Sciences Division, Oak Ridge National Laboratory, Oak Ridge, Tennessee 37831, USA; E-mail: dais@ornl.gov*

[b]*Department of Chemistry, University of Tennessee, Knoxville, Tennessee 37996, USA*

[c]*State Key Laboratory of Silicon Materials, Cyrus Tang Center for Sensor Materials and Applications, Department of Materials Science and Engineering, Zhejiang University, Hangzhou, Zhejiang 310027, P. R. China; E-mail: cuiyj@zju.edu.cn*

[d]*Center for Nanophase Materials Sciences, Oak Ridge National Laboratory, Oak Ridge, Tennessee 37831, USA*

†Electronic Supplementary Information (ESI) available: Experimental and measurements, powder XRD patterns of hierarchical MOFs, powder XRD patterns of RB@IRMOF-3 composite, nitrogen –196 ºC isotherms of RB@IRMOF-3 composite, emission spectra of RB solution in ethanol and RB@IRMOF-3 composite, fluorescence spectra of RB@IRMOF3 treated with methanol and ethanediol, the emission peak-height ratios between ligand and dye moieties, the porosity details of these hierarchical MOF series. See DOI: 10.1039/b000000x/

1 (a) L. Ma, C. Abney and W. Lin, *Chem. Soc. Rev*. **2009**, *38*, 1248–1256; (b) O. M. Yaghi, M. O'Keeffe, N. W. Ockwig, H. K. Chae, M. Eddaoudi and J. Kim, *Nature* **2003**, *423*, 705–714; (c) A. Sonnauer, F. Hoffmann, M. Fröba, L. Kienle, V. Duppel, M. Thommes, C. Serre, G. Férey and N. Stock, *Angew. Chem. Int. Ed*. **2009**, *48*, 3791–3794; (d) Z. Wang and S. M. Cohen, *Chem. Soc. Rev*. **2009**, *38*, 1315–1329; (e) G. K. H. Shimizu, R. Vaidhyanathan and J. M. Taylor, *Chem. Soc. Rev*. **2009**, *38*, 1430–1449; (f) O. K. Farha, C. E. Wilmer, I. Eryazici, B. G. Hauser, P. A. Parilla, K. O'Neill, A. A. Sarjeant, S. T. Nguyen, R. Q. Snurr and J. T. Hupp, *J. Am. Chem. Soc*. **2012**, *134*, 9860–9863.

2 (a) S.-T. Zheng, J. Zhang and G.-Y. Yang, *Angew. Chem. Int. Ed*. **2008**, *47*, 3909–3913; (b) B. Wang, W. Yao, J. Lin, Z. Ding and C. Wang, *Angew. Chem. Int. Ed*. **2014**, *53*, 1034 –1038; (c) A. N. Khlobystov, A. J. Blake, N. R. Champness, D. A. Lemenovskii, A. G. Majouga, N. V. Zyk and M. Schröder, *Coord. Chem. Rev*. **2001**, *222*, 155–192; (d) B. Moulton and M. J. Zaworotko, *Chem. Rev*. **2001**, *101*, 1629–1658; (e) J. R. Li, R.-J. Kuppler and H.-C. Zhou, *Chem. Soc. Rev*. **2009**, *38*, 1477–1504; (f) J. P. Zhang, Y. B. Zhang, J. B. Lin and X. M. Chen, *Chem. Rev*. **2012**, *112*, 1001–1033.

3 (a) M. J. Cliffe, C. Mottillo, R. S. Stein, D. K. Bučar and T. Friščić, *Chem. Sci*. **2012**, *3*, 2495–2500; (b) S. T. Zheng, T. Wu, C. T. Chou, A. Fuhr, P. Y. Feng and X. H. Bu, *J. Am. Chem. Soc*. **2012**, *134*, 1934–1937; (c) S. Bourrelly, P. L. Llewellyn, C. Serre, F. Millange, T. Loiseau and G. Férey, *J. Am. Chem. Soc*. **2005**, *127*, 13519–13521; (d) T. Ben, C. J. Lu, C. Y. Pei, S. X. Xu and S. L. Qiu, *Chem. Eur. J*. **2012**, *18*, 10250–10253; (e) K. S. Park, Z. Ni, A. P. Côté, J. Y. Choi, R. Huang, F. J. Uribe-Romo, H. K. Chae, M. O'Keeffe and O. M. Yaghi, *Proc. Natl Acad. Sci*. **2006**, *103*, 10186–10191.

4 (a) W.-Y. Gao, Y. Chen, Y. Niu, K. Williams, L. Cash, P. J. Perez, L. Wojtas, J. Cai, Y.-S. Chen and S. Ma, *Angew. Chem. Int. Ed*. **2014**, *53*, 2615–2619; (b) H. Deng, S. Grunder, K. E. Cordova, C. Valente, H. Furukawa, M. Hmadeh, F. Gándara, A. C. Whalley, Z. Liu, S. Asahina, H. Kazumori, M. O'Keeffe, O. Terasaki, J. F. Stoddart and O. M. Yaghi, *Science* **2012**, *336*, 1018–1023; (c) D. M. D'Alessandro, B. Smit and J. R. Long, *Angew. Chem. Int. Ed*. **2010**, *49*, 6058–6082.

5 (a) W. Zhang and R.-G. Xiong, *Chem. Rev*. **2012**, *112*, 1163–11195; (b) H. Furukawa, N. Ko, Y. B. Go, N. Aratani, S. B. Choi, E. Choi, A. Ö. Yazaydin, R. Q. Snurr, M. O'Keeffe, J. Kim and O. M. Yaghi, *Science* **2010**, *329*, 424–428; (c) K. Konstas, T. Osl, X. Yang, M. Batten, N. Burke, A. J. Hill and M. R. Hill, *J. Mater. Chem*. **2012**, *22*, 16698–16708; (d) H. Wu, H. Gong, D. H. Olson and J. Li, *Chem. Rev*. **2012**, *112*, 836–868; (e) W. M. Bloch, R. Babarao, M. R. Hill, C. J. Doonan and C. J. Sumby, *J. Am. Chem. Soc*. **2013**, *135*, 10441–10448; (f) Z. Chen, S. Xiang, H. D. Arman, P. Li, S. Tidrow, D. Zhao and B. Chen, *Eur. J. Inorg. Chem*. **2010**, 3745–3749.

6 (a) A. Carné-Sánchez, I. Imaz, M. Cano-Sarabia and D. Maspoch, *Nature Chem*. **2013**, *5*, 203–211; (b) A. Bétard and R. A. Fischer, *Chem. Rev*. **2012**, *112*, 1055–1083; (c) M. K. Suh, H. J. Park, T. K. Prasad and D.-W. Lim, *Chem. Rev*. **2012**, *112*, 782–835; (d) M. Yoon, R. Srirambalaji and K. Kim, *Chem. Rev*. **2012**, *112*, 1196–1231; (e) J. Kim, N. D. McNamara, T. H. Her and J. C. Hicks, *ACS Appl. Mater. Interfaces* **2013**, *5*, 11479–11487; (f) T. Lee, H. L. Lee, M. H. Tsai, S.-L. Cheng, S.-W. Lee, J.-C. Hu and L.-T. Chen, *Biosens. Bioelectron*. **2013**, *43*, 56–62; (g) L. Sun, H. Xing, Z. Liang, J. Yu and R. Xu *Chem. Commun*. **2013**, *49*, 11155–11157.

7 (a) X. Wang, S. Ma, D. Sun, S. Parkin and H.-C. Zhou, *J. Am. Chem. Soc*. **2006**, *128*, 16474–16475; (b) K. Lee, W. C. Isley, A. L. Dzubak, P. Verma, S. J. Stoneburner, L.-C. Lin, J. D. Howe, E. D. Bloch, D. A. Reed, M. R. Hudson, C. M. Brown, J. R. Long, J. B. Neaton, B. Smit, C. J. Cramer, D. G. Truhlar and L. Gagliardi, *J. Am. Chem. Soc*. **2014**, *136*, 698–704; (c) V. Lykourinou, Y. Chen, X.-S. Wang, L. Meng, T. Hoang, L.-J. Ming, R. L. Musselman and S. Ma, *J. Am. Chem. Soc*. **2011**, *133*, 10382–10385.

8 (a) M. Klimakow, P. Klobes, A. F. Thünemann, K. Rademann and F. Emmerling, *Chem. Mater*. **2010**, *22*, 5216–5221; (b) L. Song, J.

Zhang, L. Sun, F. Xu, F. Li, H. Zhang, X. Si, C. Jiao, Z. Li, S. Liu, Y. Liu, H. Zhou, D. Sun, Y. Du, Z. Cao and Z. Gabelica, *Energy Environ. Sci*. **2012**, *5*, 7508–7520; (c) S. C. Junggeburth, K. Schwinghammer, K. S. Virdi, C. Scheu and B. V. Lotsch, *Chem. Eur. J*. **2012**, *18*, 2143–2152.

9 (a) P. Horcajada, C. Serre, D. Grosso, C. Boissiére, S. Perruchas, C. Sanchez and G. Férey, *Adv. Mater*. **2009**, *21*, 1931–1935; (b) L. Li, S. Xiang, S. Cao, J. Zhang, G. Ouyang, L. Chen and C.-Y. Su, *Nat. Comms*. **2013**, *4*, 1774; (c) Y. Yue, Z.-A. Qiao, P. F. Fulvio, A. J. Binder, C. Tian, J. Chen, K. M. Nelson, X. Zhu and S. Dai, *J. Am. Chem. Soc*. **2013**, *135*, 9572–9575; (d) M. R. Lohe, M. Rose and S. Kaskel, *Chem. Commun*. **2009**, 6056–6058.

10 (a) M.-H. Pham, G.-T. Vuong, F.-G. Fontaine and T.-O. Do, *Cryst. Growth Des*. **2012**, *12*, 1008–1013; (b) Z. Xin, J. Bai, Y. Pan and M. J. Zaworotko, *Chem. Eur. J*. **2010**, *16*, 13049–13052.

11 (a) C. Liu, T. Li and N. L. Rosi, *J. Am. Chem. Soc*. **2012**, *134*, 18886–18888; (b) N. Klein, I. Senkovska, K. Gedrich, U. Stoeck, A. Henschel, U. Mueller and S. Kaskel, *Angew. Chem. Int. Ed*. **2009**, *48*, 9954–9957; (c) S. Yang, X. Lin, W. Lewis, M. Suyetin, E. Bichoutskaia, J. E. Parker, C. C. Tang, D. R. Allan, P. J. Rizkallah, P. Hubberstey, N. R. Champness, K. M. Thomas, A. J. Blake and M. Shröder, *Nat. Mater*. **2012**, *11*, 710–716; (d) P. K. Thallapally, J. Tian, M. R. Kishan, C. A. Fernandez, S. J. Dalgarno, P. B. McGrail, J. E. Warren and J. L. Atwood, *J. Am. Chem. Soc*. **2008**, *130*, 16842–16843.

12 (a) Q. Yuan, Q. Liu, W.-G. Song, W. Feng, L.-D. Sun, Y.-W. Zhang and C.-H. Yan, *J. Am. Chem. Soc*. **2007**, *129*, 6698–6699; (b) Y. Wan and D. Zhao, *Chem. Rev*. **2007**, *107*, 2821–2860; (c) S. Polarz, A. V. Orlov, F. Schüth and A.-H. Lu, *Chem. Eur. J*. **2007**, *13*, 592–597; (d) D. Zhao, Q. Huo, J. Feng, B. F. Chmelka and G. D. Stucky, *J. Am. Chem. Soc*. **1998**, *120*, 6024–6036; (e) D. Wang, D. Choi, Z. Yang, V. V. Viswanathan, Z. Nie, C. Wang, Y. Song, J.-G. Zhang and J. Liu, *Chem. Mater*. **2008**, *20*, 3435–3442.

13 L.-B. Sun, J.-R. Li, J. Park and H.-C. Zhou, *J. Am. Chem. Soc*. **2012**, *134*, 126–129.

14 (a) B. Ingham, T. H. Lim, C. J. Dotzler, A. Henning, M. F. Toney and R. D. Tilley, *Chem. Mater*. **2011**, *23*, 3312–3317; (b) K. Möler, B. Yilmaz, U. Müler and T. Bein, *Chem. Eur. J*. **2012**, *18*, 7671–7674; (c) Y. Yue, A. J. Binder, B. Guo, Z. Zhang, Z.-A. Qiao, C. Tian and S. Dai, *Angew. Chem. Int. Ed*. **2014**, *53*, 3134–3137.

15 (a) M. Eddaoudi, J. Kim, N. Rosi, D. Vodak, J. Wachter, M. O'Keeffe and O. M. Yaghi, *Science* **2002**, *295*, 469–472; (b) D. Britt, D. Tranchemontagne and O. M. Yaghi, *Proc. Natl Acad. Sci*. **2008**, *105*, 11623–11627.

16 (a) C. G. Carson, K. Hardcastle, J. Schwartz, X. Liu, C. Hoffmann, R. A. Gerhardt and A. Tannenbaum, *Eur. J. Inorg. Chem*. **2009**, 2338–2343; (b) Z. Xin, J. Bai, Y. Shen and Y. Pan, *Cryst. Growth Des*. **2010**, *10*, 2451–2454.

17 H.-K. Zhao, B. Ding, E.-C. Yang, X.-G. Wang and X.-J. Zhao, *Z. Anorg. Allg. Chem*. **2007**, *633*, 1735–1738.

18 (a) Y.-P. Zhu, T.-Z. Ren and Z.-Y. Yuan, *New J. Chem*. **2014**, *38*, 1905–1922; (b) A. Carné-Sánchez, I. Imaz, K. C. Stylianou and D. Maspoch, *Chem. Eur. J*. **2014**, DOI: 10.1002/chem.201304529.

19 (a) M.-J. Dong, M. Zhao, S. Ou, C. Zou and C.-D. Wu, *Angew. Chem. Int. Ed*. **2014**, *53*, 1575 –1579; (b) A. S. Gupta, R. K. Deshpande, L. Liu, G. I. N. Waterhouseb and S. G. Telfer, *CrystEngComm* **2012**, *14*, 5701–5704; (c) X. Zhao, X. Bu, T. Wu, S. T. Zheng, L. Wang and P. Feng, *Nat. Commun*. **2013**, *4*, 2344.

20 F. Tsunomori and H. Ushiki, *Physics Letters A* **1999**, *258*, 171–176.

21 (a) Q.-R. Fang, G.-S. Zhu, Z. Jin, Y.-Y. Ji, J.-W. Ye, M. Xue, H. Yang, Y. Wang and S.-L. Qiu, *Angew. Chem. Int. Ed*. **2007**, *46*, 6638–6642; (b) J. Yu, Y. Cui, C. Wu, Y. Yang, Z. Wang, M. O'Keeffe, B. Chen and G. Qian, *Angew. Chem. Int. Ed*. **2012**, *51*, 10542–10545; (c) J. Yu, Y. Cui, H. Xu, Y. Yang, Z. Wang, B. Chen and G. Qian, *Nat. Comms*. **2013**, *4*, 2719.

22 C. J. Doonan, W. Morris, H. Furukawa and O. M. Yaghi, *J. Am. Chem. Soc*. **2009**, *131*, 9492–9493.

TOC

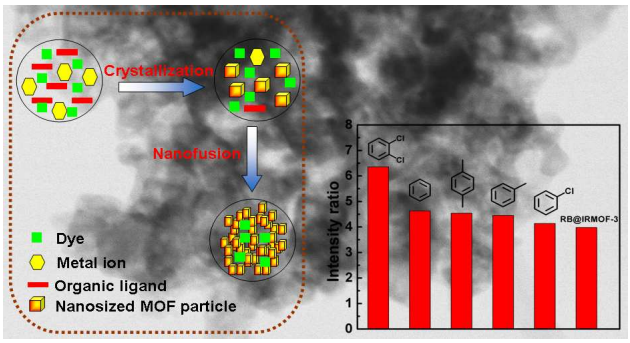

Encapsulation of Large Dye Molecules in Hierarchically Superstructured Metal-Organic Frameworks

Yanfeng Yue, Andrew J. Binder, Ruijing Song, Yuanjing Cui,* Jihua Chen, Dale K. Hensley, and Sheng Dai*

Microporous metal–organic frameworks (MOFs) represent a new family of microporous materials, offering potential applications in gas separation and storage, catalysis, and membranes. The engineering of hierarchical superstructured MOFs, i.e., fabricating mesopores in microporous frameworks during the crystallization stage is expected to serve a myriad of applications for molecular adsorption, drug delivery, and catalysis. However, MOFs with mesopores are rarely studied because of the lack of a simple, effective way to construct mesoscale cavities in the structures. Here, we report the use of a perturbation-assisted nanofusion technique to construct hierarchically superstructured MOFs. In particular, the mesopores in the MOF structure enabled the confinement of large dye species, resulting in fluorescent MOF materials, which can serve as a new type of ratiometric luminescent sensors for typical volatile organic compounds.

TOC